DOI: https://doi.org/10.17816/gc631806

TRIM29 protein partners in cultured immortalized normal basal epithelial cells of the prostate

Rinat I. Sultanov[1], Alina S. Mulyukina[1], Victoria O. Shender[1, 2], Maria M. Lukina[1], Maria A. Lagarkova[1], Georgij P. Arapidi[1, 2]

[1] Lopukhin Federal Research and Clinical Center of Physical-Chemical Medicine of Federal Medical Biological Agency, Moscow, Russia;

[2] Shemyakin & Ovchinnikov Institute of Bioorganic Chemistry of the Russian Academy of Sciences, Moscow, Russia

ABSTRACT

BACKGROUND: The E3 ubiquitin ligase TRIM29 is involved in basal epithelial development, cellular response to viral infection, and DNA damage. Furthermore, this protein can have both oncogenic and tumor suppressor properties. However, the molecular mechanisms of TRIM29 involvement in such a wide range of biological processes remain unclear.

AIM: To identify protein partners of TRIM29 and its truncated forms and to determine the key molecular processes in which it is involved.

MATERIALS AND METHODS: Cell cultures of normal prostate basal epithelium with overexpression of a full length TRIM29-FLAG chimeric protein or its truncated forms without the B-box or coiled-coil domain were obtained. Subsequently, protein partners of TRIM29 and truncated forms of TRIM29 were identified by protein immunoprecipitation followed by proteomic analysis (high-performance liquid chromatography with tandem mass spectrometry). Results were confirmed by Western blot and immunocytochemistry.

RESULTS: TRIM29 binds to 288 proteins in the normal basal epithelium of the prostate. Deletion of the B-box has little effect on TRIM29 protein-protein interactions, whereas deletion of the coiled-coil domain deprives TRIM29 of most of its protein partners and impairs its dimerization. TRIM29 was found to localize to both the nucleus and cytoplasm, while deletion of functional domains does not prevent localization to different compartments, but does affect binding to proteins specific to these compartments. TRIM29 binds to cytoskeleton proteins, cellular stress response proteins, and RNA-binding proteins. In addition, TRIM29 is shown to increase cell resistance to genotoxic agents and to affect RNA splicing.

CONCLUSION: Proteomic analysis showed that in normal prostate basal epithelium, E3 ubiquitin ligase TRIM29 binds to a relatively large number of proteins that perform different functions in different cell compartments. Our results are consistent with results obtained by other research teams who showed that TRIM29 is actively involved in cytoskeletal remodeling, cellular response to viral infection, and DNA damage. In addition, it was shown for the first time that TRIM29 interacts with stress granule proteins and RNA binding proteins and is able to regulate RNA splicing, and the coiled-coil domain of TRIM29 may play a key role in this process.

Keywords: prostate cancer; PCa; TRIM29; basal epithelium; interactome; E3 ubiquitin ligase; RNA binding proteins.

To cite this article:
Sultanov RI, Mulyukina AS, Shender VO, Lukina MM, Lagarkova MA, Arapidi GP. TRIM29 protein partners in cultured immortalized normal basal epithelial cells of the prostate. *Genes & cells.* 2024;19(4):496–512. DOI: https://doi.org/10.17816/gc631806

Received: 08.05.2024 **Accepted:** 03.08.2024 **Published online:** 27.11.2024

DOI: https://doi.org/10.17816/gc631806

Белковые партнёры TRIM29 в культуре иммортализованных клеток нормального базального эпителия предстательной железы

Р.И. Султанов[1], А.С. Мулюкина[1], В.О. Шендер[1, 2], М.М. Лукина[1], М.А. Лагарькова[1], Г.П. Арапиди[1, 2]

[1] Федеральный научно-клинический центр физико-химической медицины имени академика Ю.М. Лопухина Федерального медико-биологического агентства, Москва, Россия;

[2] Институт биоорганической химии имени академиков М.М. Шемякина и Ю.А. Овчинникова РАН, Москва, Россия

АННОТАЦИЯ

Обоснование. E3-убиквитин-лигаза TRIM29 вовлечена в развитие базального эпителия, клеточного ответа на вирусные инфекции и на повреждения ДНК. Кроме того, этот белок может проявлять как онкогенные, так и онкосупрессорные свойства. Однако до сих пор неизвестны молекулярные механизмы, обеспечивающие участие TRIM29 в столь широком спектре биологических процессов.

Цель исследования — определение белков-партнёров TRIM29 и его усечённых форм с последующим выявлением ключевых молекулярных процессов, в которые он вовлечён.

Материалы и методы. Получали клеточные культуры нормального базального эпителия предстательной железы со сверхэкспрессией химерного белка TRIM29-FLAG или его усечённых форм без B-Box-домена или без Coiled-Coil-домена. После этого определяли белки-партнёры TRIM29 и его усечённых форм при помощи иммунопреципитации белка с последующим протеомным анализом (высокоэффективная жидкостная хроматография с тандемной масс-спектрометрией). Результаты были подтверждены вестерн-блот-анализом и иммуноцитохимическим анализом.

Результаты. TRIM29 связывается с 288 белками в нормальном базальном эпителии предстательной железы. Делеция B-Box слабо влияет на белок-белковые взаимодействия TRIM29, а делеция Coiled-Coil-домена лишает TRIM29 большей части белковых партнёров и нарушает его димеризацию. Показано, что TRIM29 локализуется как в ядре, так и в цитоплазме, при этом делеция функциональных доменов не препятствует локализации в различных компартментах, но влияет на связывание с белками, специфичными для этих компартментов. TRIM29 связывается с белками цитоскелета, белками клеточного ответа на стресс и с РНК-связывающими белками. И кроме того, показано, что TRIM29 повышает устойчивость клеток к генотиксичным агентам и влияет на процесс сплайсинга РНК.

Заключение. Протеомный анализ показал, что в нормальном базальном эпителии предстательной железы E3-убиквитин-лигаза связывается с довольно большим количеством белков, выполняющих разные функции в различных компартментах клетки. Полученные результаты согласуются с результатами других исследовательских групп, показавших, что TRIM29 активно участвует в перестройке цитоскелета, клеточном ответе на вирусную инфекцию и на повреждения ДНК. Кроме того, впервые продемонстрировано, что TRIM29 взаимодействует с белками стрессовых гранул и РНК-связывающими белками и способен регулировать сплайсинг РНК, а Coiled-Coil-домен TRIM29 может играть в этом ключевую роль.

Ключевые слова: рак предстательной железы; РПЖ; TRIM29; базальный эпителий; интерактом; E3-убиквитин-лигаза; РНК-связывающие белки.

Как цитировать:
Султанов Р.И., Мулюкина А.С., Шендер В.О., Лукина М.М., Лагарькова М.А., Арапиди Г.П. Белковые партнёры TRIM29 в культуре иммортализованных клеток нормального базального эпителия предстательной железы // Гены и клетки. 2024. Т. 19, № 4. С. 496–512. DOI: https://doi.org/10.17816/gc631806

Рукопись получена: 08.05.2024 **Рукопись одобрена:** 03.08.2024 **Опубликована online:** 27.11.2024

BACKGROUND

TRIM29 is an E3 ubiquitin ligase found predominantly in the basal epithelium. This is one of the epigenetic modulators of the transcription factor TP63, the master regulator of epithelial development [1–3]. In addition, the TRIM29 protein is involved in many cellular processes, including the response to viral infection, the response to DNA damage, and the regulation of p53-dependent apoptosis. TRIM29 contributes to carcinogenesis and can manifest both oncogenic and tumor suppressor properties in various cancer types. In lung, pancreatic, bladder, stomach, liver, bone, and rectal cancers, a significant increase in *TRIM29* expression is observed in tumor tissue compared to adjacent non-tumor tissue, which correlates with an increase in cell proliferation [3–6]. TRIM29 often regulates the epithelial-to-mesenchymal transition and promotes increased cell mobility and invasion, which leads to the metastasis of tumors [3–8]. However, TRIM29 may act as a tumor suppressor in cervical, breast, prostate, and squamous cell skin cancers. Interestingly, high invasiveness, metastasis, and poor clinical prognosis in these cases are associated with low levels of *TRIM29* expression. *TRIM29* expression is regulated at the level of gene methylation [2, 3, 9, 10].

TRIM29 is a non-canonical member of the TRIM family of E3 ubiquitin ligases that lacks a catalytic RING domain. The human TRIM29 protein is 588 amino acids long and consists of three functional domains: two B-Box domains and a coiled-coil domain (Fig. 1, *a*). Unlike other members of the TRIM protein family, TRIM29 performs E3 ubiquitin ligase activity through a combination of the two B-box domains [11]. No specific domains have been found at the C-terminus of TRIM29. However, a motif has been identified that binds the MSH2 protein involved in double-strand DNA break repair [9]. Since disruption of the *TRIM29* expression program is associated with tumor development [1, 3–6], the expression of this gene can be used as a prognostic marker. Overexpression of *TRIM29* in gastrointestinal cancer is associated with a poor prognosis [3–6]. Our group has shown that in normal basal prostate epithelium, TRIM29 protein can be localized to the nucleus and interact with DNA repair system proteins such as MSH2 and MSH6 [1, 9]. In addition, *TRIM29* knockdown significantly reduces the number of foci of phosphorylated histone H2AX, a marker of double-strand DNA break repair [1]. However, information about TRIM29 protein partners in cell compartments other than the nucleus has not been fully understood. The influence of the functional domains of TRIM29 on the interactions with its protein partners (interactome) is not known.

This study evaluated the protein partners of full-length TRIM29 and the effect of its functional domains on its interactome. The coiled-coil domain is found to play a major role in protein–protein interactions, whereas the B-box domain does not have a significant effect on the TRIM29 interactome. Removal of the coiled-coil domain disrupts TRIM29 binding to nuclear proteins, particularly RNA-binding proteins. TRIM29 has been shown to be involved in responding to genotoxic stress. In addition, TRIM29 is shown for the first time to regulate RNA splicing. Therefore, TRIM29 is a potential target for a novel anti-tumor therapy due to its involvement in a variety of biological processes.

The study aimed to identify the protein partners of TRIM29 and its truncated forms, followed by evaluation of key molecular processes in which TRIM29 is involved, and to understand the effects of functional domains of TRIM29 on its protein partners.

MATERIALS AND METHODS

Cell culture. The paper used RWPE-1 (CRL-3607; ATCC, USA), Phoenix, HEK293, PC3 cell lines (obtained from the Laboratory of Cell Biology of the Lopukhin Federal Research and Clinical Center of Physical-Chemical Medicine of the Federal Medical-Biological Agency of the Russian Federation). The RWPE-1 cell line was cultured in the Keratinocyte-SFM medium (Thermo Fisher Scientific, USA). PC3, Phoenix, and HEK293 cells were cultured in the Dulbecco's Modified Eagle Medium (PanEco, Russia) supplemented with 10% fetal bovine serum. All cell cultures were incubated at 37°C with 5% CO_2.

Cells were cultured to 50% confluence before the addition of tumor necrosis factor alpha (TNF-α) (PanEco, Russia), H_2O_2 (589271809; Tula Pharmaceutical Factory, Russia), or doxorubicin (D1515; Sigma-Aldrich, USA) at 100 ng/mL, 0.1 μM, and 2 μM, respectively, and incubated for 48 hours after the addition of the active agent.

Antibodies used in this study. The following primary antibodies were used: anti-p63-alpha (13109; Cell Signaling Technology, USA), anti-TRIM29 (5182; Cell Signaling Technology, USA), anti-DYKDDDDK (anti-FLAG, 14793; Cell Signaling Technology, USA), anti-H1 (ab125027; Abcam, UK), anti-gamma H2A.X (phospho S139) (#05-636; Sigma-Aldrich, USA), anti-H3 (9715; Cell Signaling Technology, USA).

The following secondary antibodies were used: Alexa Fluor 488-conjugated (#A-11008, #A-11001; Thermo Scientific, USA), anti-mouse IgG HRP-conjugated (G-21040; Invitrogen, USA), anti-rabbit IgG HRP-conjugated (G-21234; Invitrogen, USA).

The Anti-FLAG M2 Magnetic Beads (M8823; Sigma-Aldrich, USA) were also used.

Gene engineering constructs encoding chimeric proteins TRIM29-FLAG, dBB-TRIM29-FLAG, dCC-TRIM29-FLAG, RFP-H1, GFP-TRIM29 (see Results). Table 1 shows the sequences of the primers used in the polymerase chain reaction to amplify fragments encoding TRIM29-FLAG, dBB-TRIM29-FLAG, dCC-TRIM29-FLAG, TRIM29, and H1. The study used cDNA (MINT; Evrogen, Russia) as a template. The cDNA was derived from RNA isolated from the RWPE-1 cell line (TRIzol; Thermo Fisher Scientific, USA). The resulting TRIM29-FLAG, dBB-TRIM29-FLAG, and

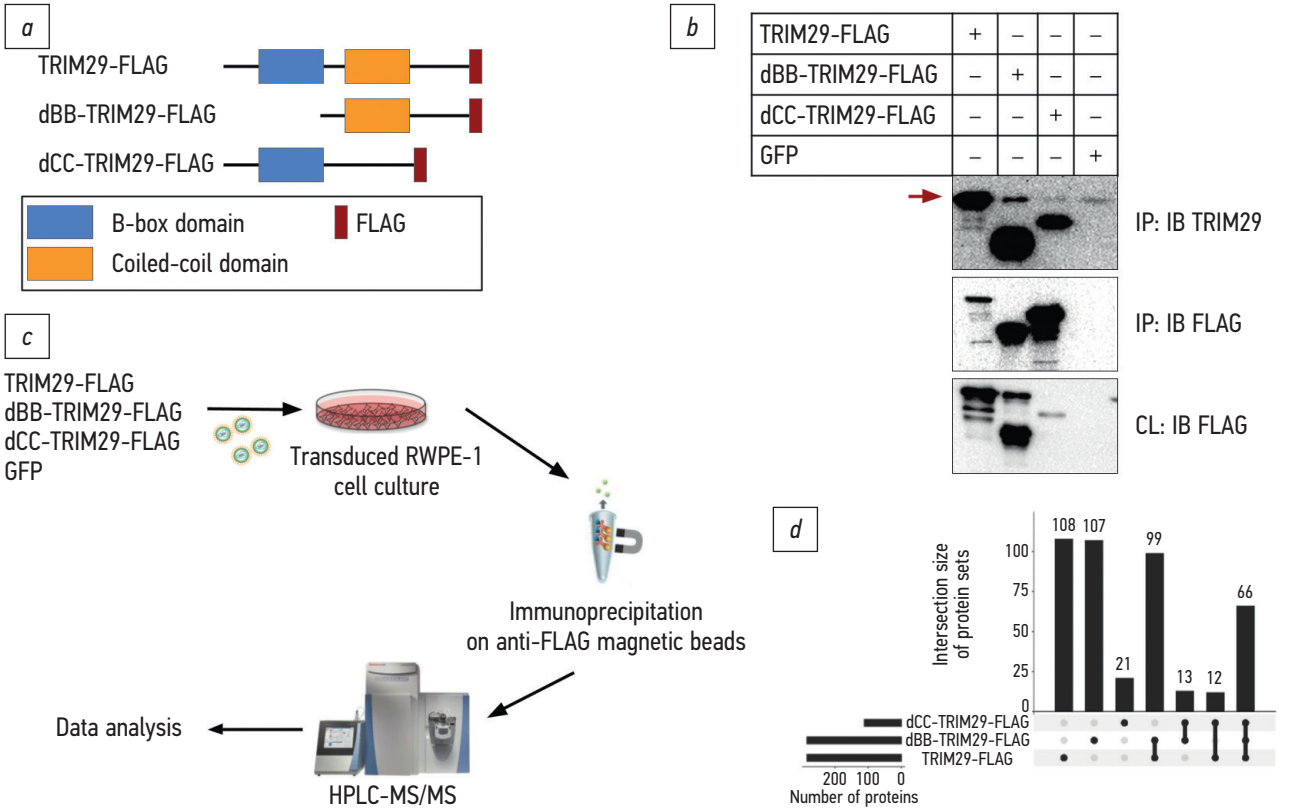

Fig. 1. Interactome of TRIM29-FLAG, dBB-TRIM29-FLAG and dCC-TRIM29-FLAG proteins in the normal prostate basal epithelial cell line RWPE-1: *a*: Domain structure of the TRIM29-FLAG protein and its truncated forms; *b*: Western blot analysis confirming the overexpression of TRIM29-FLAG and its truncated forms in the RWPE-1 cell line, results of the immunoprecipitation of TRIM29-FLAG and its truncated forms; the red arrow indicates endogenous TRIM29; *c*: Design of experiment to evaluate the interactome of the TRIM29-FLAG protein and its truncated forms; *d*: A graph showing the number of protein partners of TRIM29-FLAG and its truncated forms; protein partners unique to each form of TRIM29 and protein partners common in pairwise comparisons between forms as well as protein partners common to all three forms are shown; vertical bars between points below the bar graphs indicate the intersection of the corresponding sets; IP, immunoprecipitation eluates are evaluated; IB, immunoblotting, membrane staining with antibodies against proteins of interest; CL, cell lysate; GFP, green fluorescent protein; HPLC-MS/MS, high-performance liquid chromatography with tandem mass spectrometry.

dCC-TRIM29-FLAG fragments were inserted via BamHI and EcoRI restriction sites into the LeGO-iG2 lentiviral vector (addgene #27341), which uses green fluorescent protein (GFP) as a marker. Co-localization of H1 and TRIM29 proteins was evaluated using commercially available transient transfection vectors pTagGFP2-N and pTagRFP-N (Evrogen, Russia) containing GFP and red fluorescent protein (RFP), respectively. Fragments encoding TRIM29 and H1 proteins were inserted into constructs via BamHI and EcoRI/XbaI restriction sites, placing TRIM29 and H1 in the same reading frame as sequences encoding GFP or RFP.

The work used a plasmid encoding FLAG-ubiquitin, provided by Anna A. Kudryaeva from the Laboratory of Hormonal Regulation Proteins at the Shemyakin and Ovchinnikov Institute of Bioorganic Chemistry of the Russian Academy of Sciences. In addition, a genetically engineered construct based on the LeGO-iG2 vector encoding TRIM29, which we previously obtained, was used [1].

Production of lentiviral particles. Phoenix cells were seeded in 10 cm culture dishes at 700,000 cells per dish prior to transfection. Supporting plasmids containing the *Rev*, *RRE*, and *VSV-G* genes (15.3%, 29.8%, and 5.6% of total DNA concentration, respectively) as well as the LeGO-iG2 plasmid encoding the chimeric protein TRIM29-FLAG or its truncated forms dBB-TRIM29-FLAG and dCC-TRIM29-FLAG were used for transfection. Transfection was performed according to the manufacturer's instructions using TurboFect transfection reagent (Thermo Fisher Scientific, USA) at a ratio of 26.4 µL to 13.2 µg DNA. The supernatant containing viral particles was harvested at 24, 48, and 72 hours after transfection, filtered through a 0.45 µm pore filter, and stored at –70°C.

Establishment of cell cultures overexpressing TRIM29-FLAG, dBB-TRIM29-FLAG and dCC-TRIM29-FLAG. 100,000 cells (RWPE-1 or PC3) per well were seeded in a 6-well plate two days prior to transduction. The virus-containing culture medium was added to the cell culture with polybrene (8 µg/mL) at 3–5 virus particles per cell. After 24 hours, the medium was changed. Two days after infection, the GFP-expressing cell population was separated using a cell sorter (FACS BD Aria III; BD Biosciences, USA).

Table 1. Oligonucleotides used in the study

Name	Sequence
TRIM29_BamHI_fwd	TTGGATCCATGGAAGCTGCAGATGCC
TRIM29_FLAG_EcoRI_rev	AAGAATTCTACTTGTCATCGTCGTCCTTGTAGTCTGGGGCTTCGTTGGAC
dBB_TRIM29_BamHI_fwd	TGGATCCATGTTCCGAGACCACCAGCT
dCC_TRIM29_fwd	CATCTGCTACCTTTGCATGATGGATGCTCTGGATGAG
dCC_TRIM29_rev	CTCATCCAGAGCATCCATCATGCAAAGGTAGCAGATG
TRIM29_EcoRI_rev	AAGAATTCTATGGGGCTTCGTTGGAC
H1_BamHI_fwd	TTGGATCCATGTCGGAAACCGCTCC
H1_XbaI_rev	TTTCTAGACTACTTCTTTTTGGCAGCCG

Immunoprecipitation. The cell pellet was resuspended in chilled cell lysis buffer (50 mM Tris-HCl, pH 7.4; 150 mM NaCl, 1 mM EDTA, 0.1% NP-40, 10% glycerol, and protease inhibitors). The lysate was frozen in liquid nitrogen, thawed at room temperature and centrifuged at 16,000 rpm for 10 minutes, and the resulting supernatant was collected. The resulting cell lysate was incubated with anti-FLAG magnetic beads overnight at 4°C on a rotator. The beads were washed twice in *Tris-buffered saline* (TBS) (150 mM NaCl, 50 mM Tris-HCl, pH 7.6). The beads were then washed one time with Lysis Buffer and three times with TBS.

Proteins were eluted from the magnetic beads with the elution buffer (8 M urea, 2 M thiourea, 10 mM Tris/HCl, pH 8.0) for 2 hours on a shaker at room temperature. The beads were removed from the eluate using a magnetic separator. The resulting eluate, containing the protein partners of the study protein, was then used for either Western blotting or mass spectrometry.

Western blotting. The cell pellet was resuspended in *Laemmli buffer* and heated at 95°C for 5 minutes, and proteins were separated electrophoretically in a Mini-Protean cell (Bio-Rad, USA) using a 10% acrylamide gel in a Tris-glycine-SDS buffer system. The proteins were transferred semi-dry onto a PVDF membrane (Bio-Rad, USA) using a Trans-Blot Turbo Transfer System (Bio-Rad, USA). The membrane was incubated in a blocking solution (*phosphate-buffered saline* [PBST] +0.1% Tween-20 + 5% non-fat dried milk; Bio-Rad, USA), followed by incubation with primary antibodies overnight at 4°C. The membrane was then washed with PBST and incubated with a solution of horseradish peroxidase-conjugated secondary antibodies for 1 hour at room temperature (or overnight at 4°C). Proteins were visualized using Pierce ECL Western Blotting Substrate (Thermo Fisher Scientific, USA) and a *ChemiDoc Imaging System* (Bio-Rad, USA).

Sample preparation and tryptic peptide mass spectrometry. Samples for mass spectrometry followed by chromatography–mass spectrometry of tryptic peptides were prepared according to a previously described protocol [1]. For mass spectrometric sample preparation, *dithiothreitol* (DTT) was added to the eluates after immunoprecipitation to reduce disulfide bonds. Cysteine thiol groups were then alkylated with iodoacetamide. Trypsinolysis was performed, followed by neutralization and desalting of samples. Samples were concentrated and re-dissolved for further analysis. Peptide fractions were separated by chromatography and analyzed by mass spectrometry.

After trypsinolysis, peptide fractions were loaded onto a column (75 μm in diameter, 50 cm in length) packed with Aeris Peptide XB-C18 2.6 μm (Phenomenex, USA) in an aqueous solution containing 3% acetonitrile and 0.1% trifluoroacetic acid. Peptides were separated by nano-electrospray chromatography (Thermo Fisher Scientific, USA) using an *Ultimate 3000 Nano LC system* (Thermo Fisher Scientific, USA) coupled to a Q Exactive HF mass spectrometer (Thermo Fisher Scientific, USA). Peptides were loaded onto a column thermostated at 40°C in buffer A (0.2% formic acid in water) and eluted with a 120-minute linear gradient of 4% buffer B to 55% buffer B (0.1% formic acid, 19.9% water, and 80% acetonitrile) at a flow rate of 350 nL/min. Prior to the introduction of a new sample, the column was washed with 95% buffer B in A for 5 minutes and then equilibrated with buffer A for 5 minutes.

Mass spectrometry data were saved by automatic switching between *MS1 scan* and up to 15 MS/MS scans (topN). The target value for MS1 scans was set to 3×10^6 with a range of 300–1200 m/z (mass to charge ratio), a maximum ion injection time of 60 ms and a resolution of 60,000. Precursor ions were isolated with a window width of 1.4 m/z and a fixed first mass of 100.0 m/z. The precursor ions were fragmented using high-energy collisional dissociation in the C-trap with a normalized collision energy of 28 eV. MS/MS scans were recorded at 15,000 resolution at 400 m/z and a target ion count of 1×10^5 in the 200–2000 m/z range with a maximum ion injection time of 30 ms.

Protein partners were identified and quantified using *MaxQuant* (v.1.5.3.30) with the *Andromeda* search engine by comparison to the *UniProt Knowledgebase* (UniProtKB), human taxon, with the following parameters: parent and

fragment ion accuracies of 20 ppm and 50 ppm, respectively, trypsin as the enzyme with a single missed trypsinolysis site allowed, methionine oxidation as a potential modification, and carbamidomethylation of cysteine as a fixed modification. Confidence levels for both peptide and protein identifications were limited by a 1% *false discovery rate* (FDR) using the Benjamini–Hochberg method, determined by a targeted-decoy search strategy. For label-free quantitative analysis, label-free quantitation (LFQ) values were calculated in MaxQuant.

A protein was considered to be a partner of TRIM29 or its truncated forms if it contained more than two peptides identified by the *MaxQuant program* and if the ratio of the peptides in the experimental sample to the control was greater than two. The *clusterProfiler* software package in the *R* programming language was used to identify biological processes involving the protein partners of TRIM29 and its truncated forms [12]. The *SubcellulaRVis* software package in the *R* programming language was used to analyze the enrichment of protein partners within cellular compartments [13].

Search for alternative splicing events. RNA sequencing data from the RWPE-1 cell line with and without TRIM29 knockdown (GSE204811) were mapped to the reference genome (hg19) with gene annotation from *gencode v37* using *STAR* [14]. Alternative splicing events were identified using rMATS [15]. An alternative splicing event was considered significant if the FDR was < 0.05 and the absolute value of the inclusion difference between comparison groups was greater than 0.1. Alternative splicing analysis was visualized using the *rmats2sashimiplot* software package [15].

Immunocytochemistry. Cells were fixed with 4% paraformaldehyde for 30 minutes and washed twice with *phosphate-buffered saline* (PBS) (ECO-Service, Russia). Cell membranes were permeabilized using 0.1% Triton X-100 solution in PBS for 5 minutes. Non-specific antigens were blocked by washing cells three times for 5 minutes each with a solution of 0.1% Tween 20 in PBS followed by incubation in a blocking solution (PBS; 0.1% Tween 20; 5% FBS; 5% goat serum) for 30 minutes. Primary antibodies were then added and incubated for 2 hours at room temperature. Cells were washed from primary antibodies with 0.1% Tween 20 three times for 5 minutes each. A solution of secondary antibodies labeled with an Alexa Fluor 555 fluorophore in PBS was added and incubated for 1 hour in the dark at room temperature. Cells were washed from secondary antibodies with 0.1% Tween 20 three times for 5 minutes each. Cell nuclei were stained by incubating cells with DAPI (100 ng/mL) for 10 minutes in the dark at room temperature. The cells were then washed once with PBS, and PBS was removed. Glycerol was added to the sample, and it was covered with a coverslip. Stained proteins were visualized using an Eclipse Ni-E fluorescence microscope (Nikon, Japan).

Confocal microscopy. Images were captured using a *Nikon A1* inverted confocal microscope with a Nikon Plan Apo 40× objective (NA 0.95) and NIS-Elements software (Nikon, Japan). The fluorescent signal for GFP/RFP was obtained using a laser with a wavelength of 488 nm and 561 nm, respectively. The emission signal for GFP/RFP was detected in the ranges of 500–550 nm and 570–620 nm, respectively.

RESULTS

Deletion of the TRIM29 coiled-coil domain was found to significantly reduce the number of its protein-protein partners in normal prostate basal epithelium

To evaluate the interactome of TRIM29 and its truncated forms in normal prostate basal epithelium, cell cultures of RWPE-1 transduced with lentiviral particles were used for overexpression of the following chimeric proteins: full-length protein TRIM29-FLAG; truncated form of TRIM29 without the region of 1–200 amino acid sequence containing the B-box domain (dBB-TRIM29-FLAG); truncated form of TRIM29 without the region of 248–352 amino acid sequence containing the coiled-coil domain (dCC-TRIM29-FLAG) (Fig. 1, *a*, *b*). Interactomes for the study proteins were obtained by immunoprecipitation with FLAG peptide-specific antibodies, followed by mass spectrometry of the precipitated samples (Fig. 1, *c*). As a negative control, the RWPE-1 cell line expressing *gfp* was used. The first thing we found was that the precipitate from dBB-TRIM29-FLAG contains full-length endogenous TRIM29 produced by RWPE-1 cells, whereas it is absent in the precipitate from dCC-TRIM29-FLAG (Fig. 1, *b*, red arrow). Therefore, deletion of the coiled-coil domain, but not the B-box domain of TRIM29, disrupts TRIM29 dimerization (Fig. 1, *b*).

For TRIM29-FLAG, dBB-TRIM29-FLAG, and dCC-TRIM29-FLAG, mass spectrometry identified 288, 288, and 113 protein partners, respectively (see Supplement 1, Fig. 1, *d*). The data show that deletion of the coiled-coil domain results in a loss of TRIM29's ability to dimerize. In addition, a significant decrease in the number of protein partners for TRIM29 was observed upon deletion of the coiled-coil domain. However, the protein partner lists of TRIM29-FLAG and dBB-TRIM29-FLAG show a significant overlap (Supplement 1). This significant overlap in the protein partner lists of TRIM29-FLAG and dBB-TRIM29-FLAG may be due to the fact that dBB-TRIM29-FLAG also binds to endogenous full-length TRIM29 in normal basal prostate epithelial cells (Fig. 1, *b*), confounding the observed pattern of its protein-protein interactions.

Effects of functional TRIM29-FLAG domains on intracellular TRIM29-FLAG localization

Analysis of the identified proteins showed that the partners of TRIM29-FLAG and dBB-TRIM29-FLAG are significantly represented in the cytoplasm, cytoskeleton,

DOI: https://doi.org/10.17816/gc631806

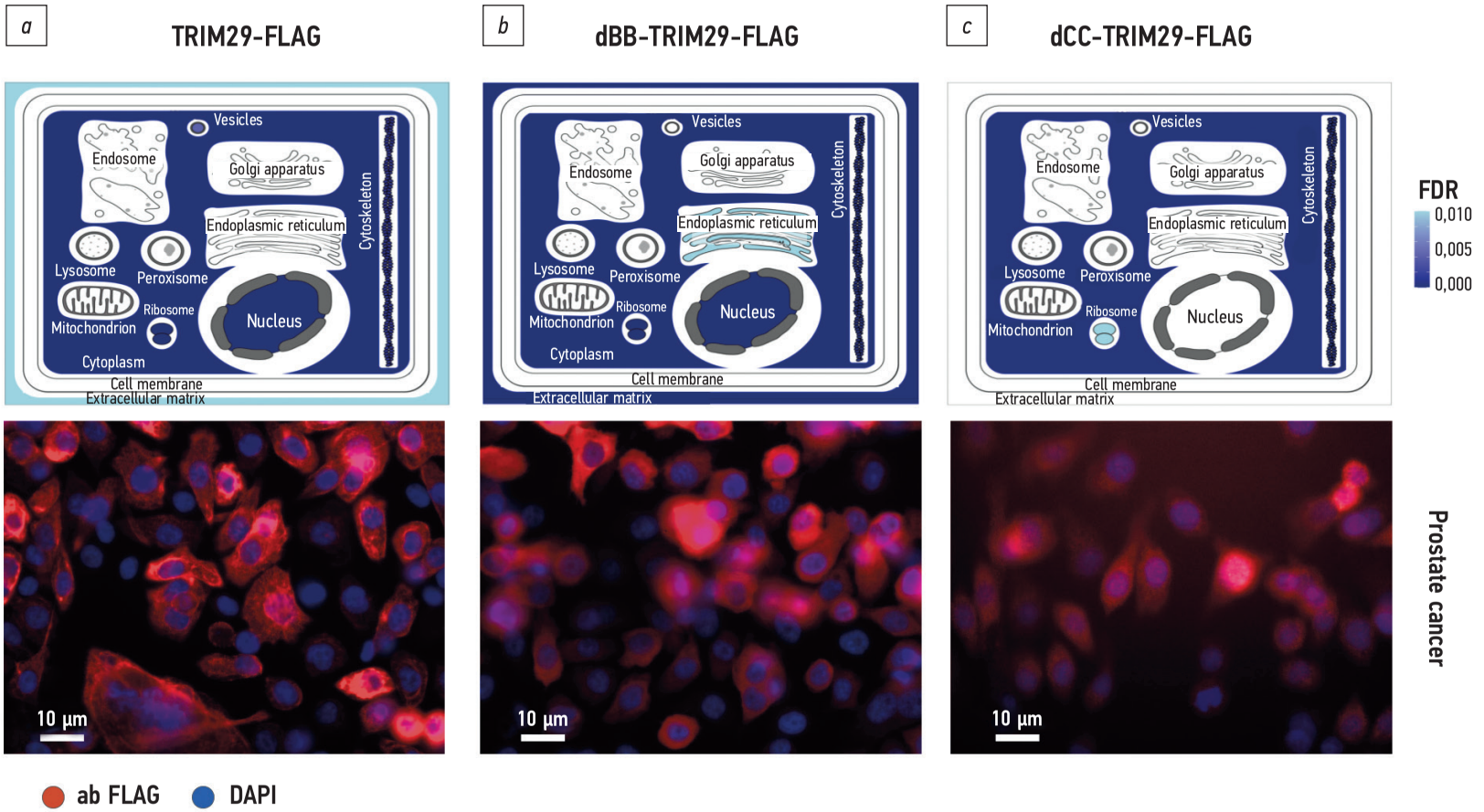

Fig. 2. Effects of functional TRIM29-FLAG domains on intracellular TRIM29-FLAG localization: Top panel: Localization of TRIM29-FLAG partner proteins and their truncated forms in cell compartments; the more intense the staining, the more significant the enrichment of the TRIM29-FLAG interactome or its truncated forms with proteins of the corresponding compartment; Bottom panel: Immunocytochemical staining with antibodies specific for the FLAG peptide (indicated in red) of PC3 cell cultures overexpressing TRIM29-FLAG or its truncated forms; nuclei are stained blue (DAPI); vertical panels correspond to overexpression of the full-length TRIM29-FLAG protein and its truncated forms of dBB-TRIM29-FLAG and dCC-TRIM29-FLAG; FDR—false discovery rate.

ribosomes, nucleus and, interestingly, in the extracellular matrix and cell vesicles (Fig. 2, *a*, *b*, *upper panel*). Deletion of the coiled-coil domain results in an interactome of TRIM29 that is depleted of nuclear proteins, ribosomal proteins, cell vesicles, and extracellular matrix proteins (Fig. 2, *c*, *upper panel*). To confirm the localization of TRIM29-FLAG, cell cultures of PC3 (prostate cancer cells lacking endogenous *TRIM29* expression) overexpressing *TRIM29-FLAG* and its truncated forms were obtained and immunocytochemistry was performed with staining by FLAG-specific antibodies. The cell nucleus was stained with DAPI (Fig. 2, *lower panel*). The figure shows that full-length TRIM29-FLAG localizes to both the cytoplasm and the nucleus. The staining pattern suggests that TRIM29-FLAG in the cytoplasm is associated with cytoskeletal proteins, which is consistent with the results of other research teams [10] and our team's immunoprecipitation data, where the largest number of identifications were found for cytoskeletal proteins (filamin, actin, myosin, tropomyosin, and tubulin; Supplement 1). For dBB-TRIM29-FLAG, a more diffuse staining and a loss of binding specificity to the cytoskeleton were observed. However, many cytoskeletal proteins were found among its protein partners (Fig. 2, *b*, *lower panel*; Supplement 1). For dCC-TRIM29-FLAG, uniform cell staining was observed with no specific affinity for any compartment (Fig. 2, *c*, lower panel). Therefore, deletion of either the B-box or the coiled-coil domain does not affect FLAG trafficking to the nucleus, but loss of the coiled-coil domain causes TRIM29-FLAG to lose its ability to bind to certain classes of nuclear proteins, such as histone H1 or spliceosome proteins, as shown by mass spectrometry (Supplement 1).

Role of TRIM29 in protein ubiquitination

Most TRIM family proteins have E3-ubiquitin ligase activity due to the RING domain [16]. However, noncanonical TRIM proteins without the ubiquitin ligase RING domain (e.g. TRIM29) can still participate in ubiquitination processes either directly via the B-box domain or by binding to other ubiquitin ligases [11, 17]. Among the protein partners of TRIM29 in normal prostate basal epithelium, ubiquitin and several E3 ubiquitin ligases such as RNF213 and HERC6 were found, which have ubiquitin ligase activity due to their canonical RING and HECT domains (Supplement 1). Interestingly, deletion of the B-box domain increases the number of TRIM family ubiquitin ligases (TRIM47, TRIM32) that bind to TRIM29, but deletion of the coiled-coil domain appears to disrupt heterodimerization of TRIM29 with other E3 ubiquitin ligases (Supplement 1). This is consistent with results from another team [16] showing that the coiled-coil domain is required for interactions with other members of the TRIM family. No E1-ubiquitin-activating enzymes or E2-ubiquitin-conjugating enzymes were found among the protein partners of full-length TRIM29. However, dBB-TRIM29-FLAG is bound to the E2-ubiquitin conjugating enzyme UBE2N, which is part of the UBE2N:UBE2V1 dimer that catalyzes K63-linked polyubiquitination that does not lead to proteasomal degradation of proteins [18]. In addition, TRIM29 was found to interact with the deubiquitinase USP10, which regulates TP53 ubiquitination levels and is involved in the cellular response to DNA damage through the TP53-dependent pathway [19]. An *in vivo* ubiquitination assay was performed by transfecting HEK293 cells with gene constructs encoding FLAG-ubiquitin and TRIM29 hybrid proteins to test how TRIM29 affects protein ubiquitination in general (see *Materials and Methods*). Protein immunoprecipitation was then performed using FLAG-specific antibodies. Western blotting of the precipitate showed that the presence of TRIM29 significantly increased the fraction of ubiquitinated proteins (Fig. 3, *a*). This may indicate that TRIM29 directly ubiquitinates many proteins or that it serves as a scaffold for other ubiquitin ligases identified among its protein partners (Supplement 1).

Role of TRIM29 in different types of responses to cellular stress

Analysis of the interactome of TRIM29-FLAG revealed that TRIM29 is involved in many biological processes related to cellular responses to various external stresses. Previous studies showed that TRIM29 is involved in the cellular response to viral infections [9, 11, 20] (Fig. 3, *b*). Among the protein partners of TRIM29, another member of the TRIM family, TRIM14, was discovered, which plays a critical role in the immune response to viral and bacterial infections [21, 22]. In addition, TRIM29 interacts with the key transcription factor STAT1. Upon stimulation by pro-inflammatory cytokines, STAT1 is phosphorylated and activates the expression of genes involved in the antiviral response [23–25]. In addition to STAT1, TRIM29 interacts with other interferon-induced proteins such as IFIT1, IFI16 and EIF2AK2. Interestingly, neither deletion of the B-box domain nor deletion of the coiled-coil domain completely eliminates association with this group of proteins. Therefore, all functional domains and unstructured regions of TRIM29 may be required for full participation in antiviral activity.

Among the partner proteins of the full-length TRIM29 FLAG, proteins involved in stress granule assembly were found according to the Gene Ontology database of biological processes (Supplement 2). The lists of the stress granule proteins from the thermal shock stress granule assembly study [26] were then compared with TRIM29 protein partners. The interactome of both full-length TRIM29-FLAG and its truncated forms were found to be significantly enriched by stress granule proteins (Fig. 3, *c*). However, such a significant enrichment could be due to cytoskeletal proteins such as MYH10, MYO1B, MYO6 and TMP1, which are present in stress granules and to which TRIM29 binds. In addition, many RNA-binding proteins from the TRIM29 interactome such as HNRNPR, HNRNPD, MATR3, and PABPC4 are also present in stress granules. Therefore, the direct involvement of TRIM29 in granule formation requires further research.

Vol. 19 (4) 2024

DOI: https://doi.org/10.17816/gc631806

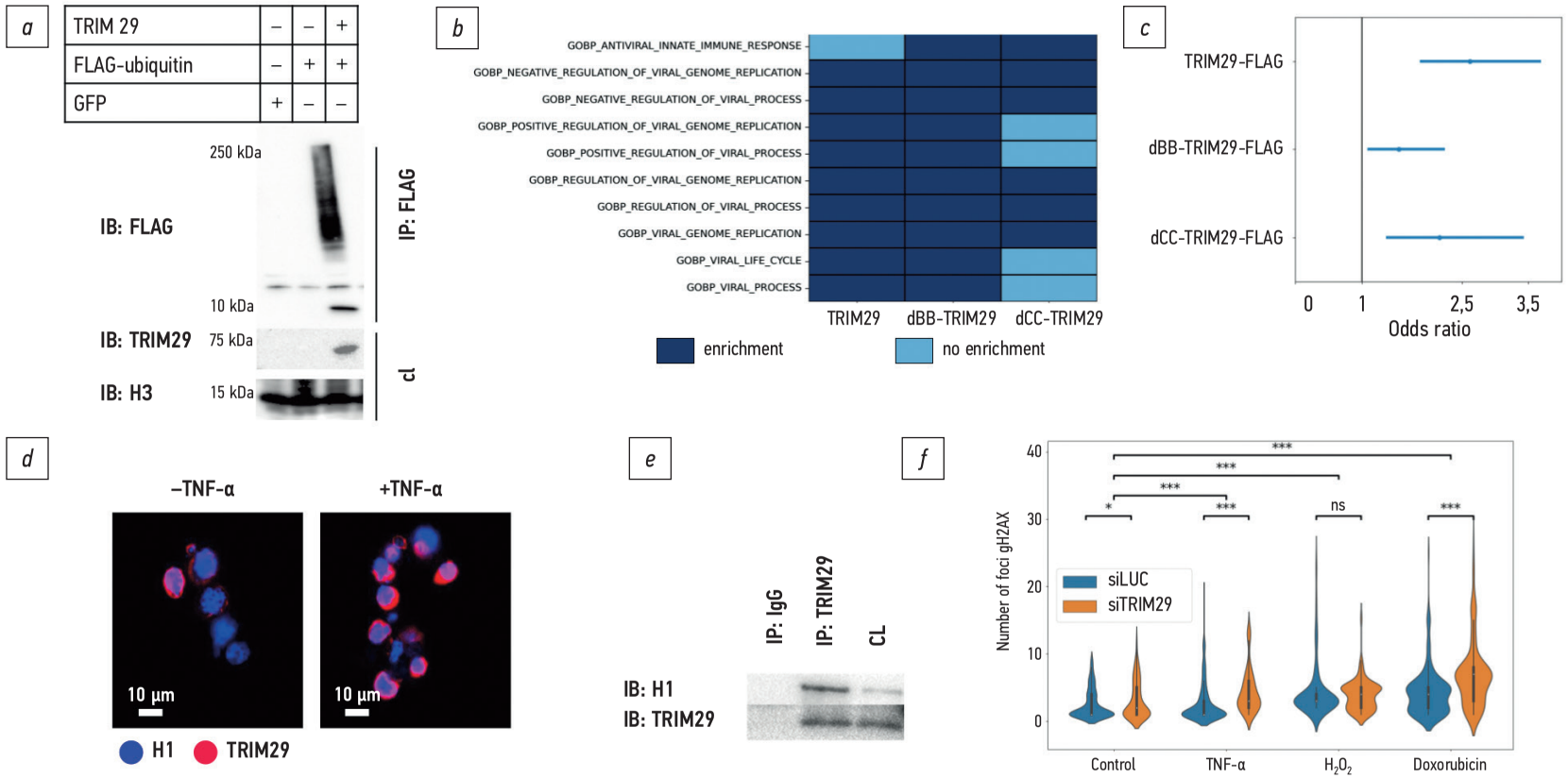

Fig. 3. TRIM29 is involved in the cellular response to stress: *a*: *In vitro* ubiquitination of proteins of the HEK293 cell line; western blot analysis of the FLAG-ubiquitin immunoprecipitate in the absence and in the presence of TRIM29; *b*: Heat map of biological pathways of cellular response to viral infection involving partner proteins and truncated forms of TRIM29-FLAG; *c*: Enrichment of partner proteins and truncated forms of TRIM29-FLAG in stress granule proteins; the vertical bar is the cut-off for the significance of the odds ratio Fisher's exact test), which should not be crossed by the confidence intervals; *d*: Confocal microscopy of HEK293 cell culture overexpressing RFP-H1 and GFP-TRIM29 in the presence of TNF-α (+TNF-α; TNF-α, 100 ng/mL, 48 h) and in the absence of TNF-α (–TNF-α); RFP-H1 localization is blue, GFP-TRIM29 localization is pink; *e*: Western blot analysis of TRIM29-FLAG immunoprecipitate using histone H1 specific antibodies in the RWPE-1 TRIM29-FLAG cell line; *f*: The number of gH2AX foci in the nucleus of RWPE-1 cell line with and without TRIM29 knockdown affected by inflammatory (TNF-α, 100 ng/mL, 48 h), oxidative (H2O2, 0.1 μM, 48 h) and genotoxic (doxorubicin, 2 μM, 48 h) stress; ns, no significant differences; * $p < 0.05$; *** $p < 1e{-}5$; IP, immunoprecipitation eluates are evaluated; IB, immunoblotting, membrane staining with antibodies against proteins of interest; CL, cell lysate; siTRIM29, TRIM29 knockdown, siLUC; knockdown control.

The role of TRIM29 in DNA repair is of particular interest. Our team has previously shown that TRIM29 significantly reduces the genotoxic effects of inflammatory stress in prostate cancer [1]. Immunoprecipitation of TRIM29 from the nuclear fraction of the RWPE-1 cell line and subsequent mass spectrometry revealed that TRIM29 interacts with proteins of the DNA repair system, including proteins involved in nucleotide excision repair (RAD23B, CENT2, DDB1), mismatch repair (MSH2, MSH6), and the TP53BP1 protein of the non-homologous end-joining family [1, 9]. In addition, TRIM29 binds to histone H1, whose ubiquitination is a marker of DNA repair [27] (Supplement 1). Therefore, TRIM29 could be a potential E3 ubiquitin ligase for H1 or an E4 ligase that ensures the interaction of another E3 ubiquitin ligase with H1. To evaluate the co-localization of these two proteins, the hybrid proteins RFP-H1 and GFP-TRIM29 were overexpressed in the HEK293 cell line using the gene constructs pTagRFP-N and pTagGFP2-N, respectively (see *Materials and Methods*). The red and green fluorescent proteins fused to H1 and TRIM29, respectively, help visualize the location of these proteins in the cell using confocal microscopy. Under inflammatory stress (TNF-α: 100 ng/mL, 48 hours), the co-localization of TRIM29 and histone H1 was shown to increase significantly (Fig. 3, *d*). In addition, the interaction between TRIM29 and H1 was confirmed by immunoprecipitation of TRIM29-FLAG followed by Western blotting of the precipitate with H1-specific antibodies (Fig. 3, *e*). We also showed that *TRIM29* knockdown in the normal prostate basal epithelium under inflammatory stress (TNF-α: 100 ng/mL for 48 hours), oxidative stress (H_2O_2: 0.1 μM for 48 hours), and genotoxic stress (doxorubicin: 2 μM for 48 hours) significantly increased the number of γH2AX foci, which are markers of DNA damage (Fig. 3, *f*). Taken together, these data demonstrate that TRIM29 plays a critical role in cellular responses to various forms of stress.

TRIM29 as protein partner of RNA-binding proteins

TRIM29 protein partners include many proteins involved in splicing, such as FXR1, FXR2, SRSF1, SRSF5, THRAP3, WBP11, HNRNPR, TCERG1, TRA2B, RBMX, and PRMT1 (Supplement 1). In addition, our analysis showed that TRIM29 binds to proteins that stabilize and transport mRNA from the nucleus, such as ELAVL1, PRRC2C, and PABPC4 (Supplement 1). However, TRIM29 itself does not have any known RNA binding domains like TRIM25, which is another member of the TRIM family [28]. This suggests that TRIM29 may be involved in the regulation of splicing either as a scaffold protein within the spliceosome or through regulation of the stability of splicing proteins. Immunoprecipitation data show that deletion of the B-box domain of TRIM29 does not affect binding to spliceosome proteins, whereas deletion of the coiled-coil domain almost completely eliminates interactions with RNA-binding proteins (Supplement 1 and Supplement 2, Fig. 4). To evaluate the effects of TRIM29 on the splicing process, we analyzed RNA-sequencing data of *TRIM29* knockdown in the normal prostate basal epithelial cell line RWPE-1 previously obtained by our team [1]. In fact, TRIM29 knockdown resulted in 35 exon skipping events and 11 intron retaining events (Fig. 5). These alternative splicing

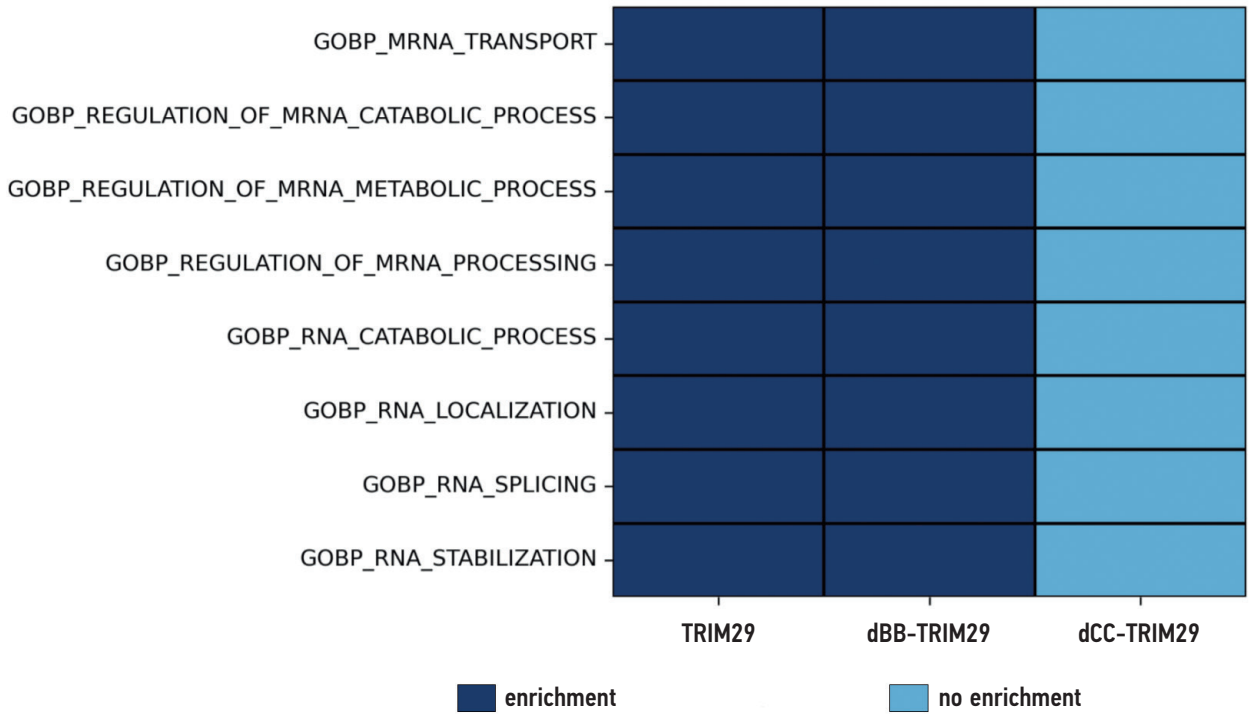

Fig. 4. Heatmap shows RNA processing biological pathways enriched with protein partners of TRIM29-FLAG and its truncated forms.

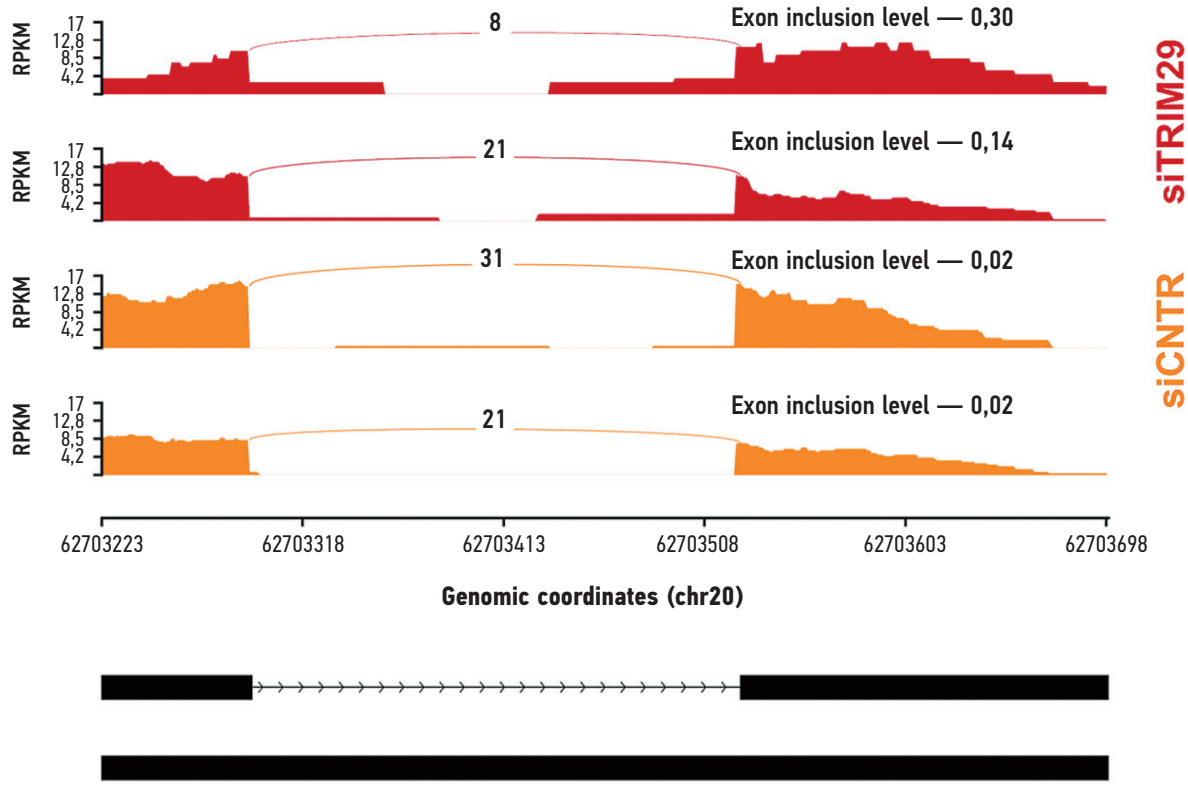

Fig. 5. Heatmap shows RNA processing biological pathways enriched with protein partners of TRIM29-FLAG and its truncated forms. siTRIM29—knockdown TRIM29, siCNTR—knockdown control, RPKM—reads per kilobase million.

events are enriched with RNA-binding protein motifs such as SRSF1, SRSF7, MATR3, PABPC4, FXR1, FXR2, HNRNPL, and IGF2BP3, which bind full-length TRIM29-FLAG or dBB-TRIM29-FLAG, but not bind dCC-TRIM29-FLAG (RNA motif enrichment data were obtained from the MAPS2 online service [29]). These data suggest that TRIM29 may play a key role in RNA splicing.

DISCUSSION

TRIM29 is a non-canonical member of the TRIM family of E3 ubiquitin ligases, which are found predominantly in the basal epithelium and have numerous functions, including the repair of double-strand DNA breaks [9, 30, 31]. The multiple functions of TRIM29 are due to its involvement in different regulatory pathways. TRIM29 responds to DNA damage by interacting with histones and recruiting repair proteins such as MSH2, MSH6, MLH1, BRCA1, ATM, the TIP60 complex, and the ubiquitin ligase RNF8 [9, 30], as confirmed by our team [1]. The identified protein partners of TRIM29 include vimentin (a marker of mesenchymal cells), heat shock protein 70, ribosomal proteins, and MARCKS (myristoylated alanine-rich C-kinase substrate involved in exocytosis) [30, 32]. TRIM29 is able to affect the distribution of keratin in the cytoplasm, thereby altering cell shape and mobility [10]. In addition, TRIM29 is shown to interact with proteins involved in antiviral responses and acts as an E3 ubiquitin ligase to promote proteasome-mediated degradation of these proteins [11, 33].

Unlike other members of the TRIM family, TRIM29 lacks a RING ubiquitin ligase domain and instead consists of two B-box (zinc finger) domains and a coiled-coil domain. Some works show that B-box domains can act as ubiquitin ligase domains [11, 34], whereas the coiled-coil domain often facilitates dimerization of TRIM proteins [16, 30]. However, the effect of these domains on TRIM29's protein partners remains poorly understood.

Our work evaluated the major biological pathways involving full-length TRIM29 and its truncated forms without B-box and coiled-coil domains, individually tested in the normal prostate basal epithelium. In contrast to deletion of the B-box domain, deletion of the coiled-coil domain was found to play a key role in TRIM29 homodimerization. Mass spectrometry of immunoprecipitates showed that the coiled-coil domain was responsible for most of the protein interactions of TRIM29, whereas loss of the B-box domain did not significantly affect the number of protein partners. The coiled-coil domain was found to play a critical role in binding to nuclear proteins, although immunocytochemical analysis of the intracellular dCC-TRIM29 FLAG position confirmed that TRIM29 can also enter the nucleus without the coiled-coil domain. This suggests that the coiled-coil domain is not mandatory for the nuclear TRIM29 position, but is required for intranuclear protein-protein interactions.

These findings confirm previous reports [9, 30] that TRIM29 is involved in cellular responses to various stress stimuli. TRIM29 binds to both antiviral response proteins and DNA repair system proteins. However, deletion of the B-box or coiled-coil domains did not prevent TRIM29's involvement in these biological pathways. We also confirmed that *TRIM29* knockdown in normal prostate basal epithelial cells reduces their ability to repair DNA.

For the first time, the interactomes of both full-length and truncated forms of TRIM29 were shown to be significantly enriched by stress granule proteins. Deletion of the B-box domain reduced binding to stress granules, which was not observed with deletion of the coiled-coil domain. As an E3 ubiquitin ligase, TRIM29 may be involved in the formation of stress granules.

Even in the absence of the canonical ubiquitin ligase domains, TRIM29 acts as an E3 ubiquitin ligase for at least NEMO and STING proteins, which are involved in the immune response to viral infections [11, 35]. Our findings show that TRIM29 interacts with a large number of ubiquitin ligases of the TRIM and other families. We also found that overexpression of TRIM29 significantly increased overall protein ubiquitination levels in HEK293 cells. This confirms the involvement of TRIM29 in ubiquitination regulation, although it remains unclear which of the identified protein partners are the actual targets for TRIM29 as an E3 ubiquitin ligase.

Analysis of the TRIM29 interactome reveals its partnership with RNA-binding proteins involved in RNA stabilization and splicing. *TRIM29* knockdown found to result in exon skips and intron retentions in the normal prostate basal epithelium. However, the regions of these alternative splicing events are enriched by binding sites of spliceosomal proteins with which TRIM29 interacts. In contrast to the B-box domain, deletion of the coiled-coil domain completely eliminates the enrichment of the TRIM29 interactome with RNA-binding proteins. This suggests that TRIM29 may participate in RNA processing not as an E3 ubiquitin ligase, but as a scaffold or stabilizing protein.

CONCLUSION

Mass spectrometry of the TRIM29 interactome showed that in the normal prostate basal epithelium, the E3 ubiquitin ligase TRIM29 binds to 288 proteins that perform various functions in different cellular compartments. Our results are consistent with results obtained by other research teams who showed that TRIM29 is actively involved in cytoskeletal remodeling, cellular response to viral infection, and DNA damage. In addition, our team shows for the first time that TRIM29 interacts with stress granule proteins and RNA-binding proteins that are involved in both mRNA stabilization and splicing, and that the coiled-coil domain of TRIM29 plays a key role in these interactions.

ADDITIONAL INFORMATION

Supplement 1. Mass spectrometry of TRIM29 FLAG interactome and its truncated forms. Accession_Number: Uniprot protein identifier, Molecular_Weight: molecular weight of protein, GFP: number of peptide identifications for the corresponding protein in the GFP-overexpressing sample, TRIM29: number of peptide identifications for the corresponding protein in the TRIM29-FLAG-overexpressing sample, dBB-TRIM29: number of peptide identifications for the corresponding protein in dBB-TRIM29-FLAG-overexpressing sample, dCC-TRIM29: number of peptide identifications for the corresponding protein in dCC-TRIM29-FLAG-overexpressing sample, Gene_Name: gene name of the corresponding protein, Description: description of protein and its functions.

https://doi.org/10.17816/gc631806-4224384

Supplement 2. Enrichment analysis of protein partners of TRIM29-FLAG and its truncated forms based on biological processes from the Gene Ontology database. Cluster: comparison group (samples overexpressing TRIM29-FLAG, dBB-TRIM29-FLAG, dCC-TRIM29-FLAG), ID: biological pathway identifier, GeneRatio: number of proteins detected from the pathway / total number of proteins in the pathway, BgRatio: number of proteins not detected from the pathway / total number of proteins, *p*value: *p*-value of hypergeometric distribution, *p*.adjust: *p*-value corrected for multiple comparisons (Benjamin–Hochberg), geneID: list of genes detected from the pathway, Count: number of proteins detected from the pathway.

https://doi.org/10.17816/gc631806-4224385

Funding source. The work was supported by the Russian Science Foundation, agreement N. 22-75-00129 "Molecular mechanism of regulation of TP63-dependent transcriptional networks through tissue-specific ubiquitin ligase TRIM29. New opportunities for the therapy of TP63-dependent types of cancer".

Competing interests. The authors declare that they have no competing interests.

Authors' contribution. R.I. Sultanov, A.S. Mulyukina — conducting research and analyzing data, writing an article; M.M. Lukina — immunocytochemical analysis; V.O. Shender — preparation of samples for mass spectrometry; M.A. Lagarkova, G.P. Arapidi — organization and conduction of research.

REFERENCES

1. Sultanov R, Mulyukina A, Zubkova O, et al. TP63-TRIM29 axis regulates enhancer methylation and chromosomal instability in prostate cancer. *Epigenetics Chromatin*. doi: 10.1186/s13072-024-00529-7

2. Masuda Y, Takahashi H, Hatakeyama S. TRIM29 regulates the p63-mediated pathway in cervical cancer cells. *Biochim Biophys Acta*. 2015;1853(10 Pt A):2296–2305. doi: 10.1016/j.bbamcr.2015.05.035

3. Palmbos PL, Wang Y, Bankhead Iii A, et al. ATDC mediates a TP63-regulated basal cancer invasive program. *Oncogene*. 2019;38(18):3340–3354. doi: 10.1038/s41388-018-0646-9

4. Han Q, Sun ML, Liu WS, et al. Upregulated expression of ACTL8 contributes to invasion and metastasis and indicates poor prognosis in colorectal cancer. *Onco Targets Ther*. 2019;12:1749–1763. doi: 10.2147/OTT.S185858

5. Du H, Xu Q, Xiao S, et al. MicroRNA-424-5p acts as a potential biomarker and inhibits proliferation and invasion in hepatocellular carcinoma by targeting TRIM29. *Life Sci*. 2019;224:1–11. doi: 10.1016/j.lfs.2019.03.028

6. Qiu F, Xiong JP, Deng J, Xiang XJ. TRIM29 functions as an oncogene in gastric cancer and is regulated by miR-185. *Int J Clin Exp Pathol*2015;8(5):5053–5061.

7. Wang L, Yang H, Abel EV, et al. ATDC induces an invasive switch in KRAS-induced pancreatic tumorigenesis. *Genes Dev*. 2015;29(2):171–183. doi: 10.1101/gad.253591.114

8. Tang ZP, Dong QZ, Cui QZ, et al. Ataxia-telangiectasia group D complementing gene (ATDC) promotes lung cancer cell proliferation by activating NF-κB pathway. *PLoS One*. 2013;8(6):e63676. doi: 10.1371/journal.pone.0063676

9. Masuda Y, Takahashi H, Sato S, et al. TRIM29 regulates the assembly of DNA repair proteins into damaged chromatin. *Nat Commun*. 2015;6:7299. doi: 10.1038/ncomms8299

10. Yanagi T, Watanabe M, Hata H, et al. Loss of TRIM29 Alters keratin distribution to promote cell invasion in squamous cell carcinoma. *Cancer Res*. 2018;78(24):6795–6806. doi: 10.1158/0008-5472.CAN-18-1495

11. Xing J, Weng L, Yuan B, et al. Identification of a role for TRIM29 in the control of innate immunity in the respiratory tract. *Nat Immunol*. 2016;17(12):1373–1380. doi: 10.1038/ni1216-1479a Corrected and republished from: *Nat Immunol*. 2016;17(12):1479. doi: 10.1038/ni.3580

12. Wu T, Hu E, Xu S, et al. clusterProfiler 4.0: A universal enrichment tool for interpreting omics data. *Innovation (Camb)*. 2021;2(3):100141. doi: 10.1016/j.xinn.2021.100141

13. Watson J, Smith M, Francavilla C, Schwartz JM. SubcellulaRVis: a web-based tool to simplify and visualise subcellular compartment enrichment. *Nucleic Acids Res*. 2022;50(W1):W718–W725. doi: 10.1093/nar/gkac336

14. Dobin A, Davis CA, Schlesinger F, et al. STAR: ultrafast universal RNA-seq aligner. *Bioinformatics*. 2013;29(1):15–21. doi: 10.1093/bioinformatics/bts635

15. Shen S, Park JW, Lu ZX, et al. rMATS: robust and flexible detection of differential alternative splicing from replicate RNA-Seq data. *Proc Natl Acad Sci U S A*. 2014;111(51):E5593–E5601. doi: 10.1073/pnas.1419161111

16. Meroni G, Diez-Roux G. TRIM/RBCC, a novel class of "single protein RING finger" E3 ubiquitin ligases. *Bioessays*. 2005;27(11):1147–1157. doi: 10.1002/bies.20304

17. Sardiello M, Cairo S, Fontanella B, et al. Genomic analysis of the TRIM family reveals two groups of genes with distinct evolutionary properties. *BMC Evol Biol*. 2008;8:225. doi: 10.1186/1471-2148-8-225

18. Cardamone MD, Krones A, Tanasa B, et al. A protective strategy against hyperinflammatory responses requiring the nontranscriptional actions of GPS2. *Mol Cell*. 2012;46(1):91–104. doi: 10.1016/j.molcel.2012.01.025

19. Yuan J, Luo K, Zhang L, et al. USP10 regulates p53 localization and stability by deubiquitinating p53. *Cell*. 2010;140(3):384–396. doi: 10.1016/j.cell.2009.12.032

20. Wikiniyadhanee R, Lerksuthirat T, Stitchantrakul W, et al. TRIM29 is required for efficient recruitment of 53BP1 in response to DNA double-strand breaks in vertebrate cells. *FEBS Open Bio*. 2020;10(10):2055–2071. doi: 10.1002/2211-5463.12954

21. Tan G, Xu F, Song H, et al. Identification of TRIM14 as a type I IFN-stimulated gene controlling hepatitis B virus replication by targeting HBx. *Front Immunol*. 2018;9:1872. doi: 10.3389/fimmu.2018.01872

22. Hoffpauir CT, Bell SL, West KO, et al. TRIM14 Is a key regulator of the type I IFN response during mycobacterium tuberculosis infection. *J Immunol*. 2020;205(1):153–167. doi: 10.4049/jimmunol.1901511

23. Liu B, Liao J, Rao X, et al. Inhibition of Stat1-mediated gene activation by PIAS1. *Proc Natl Acad Sci U S A*. 1998;95(18):10626–10631. doi: 10.1073/pnas.95.18.10626

24. DeVries TA, Kalkofen RL, Matassa AA, Reyland ME. Protein kinase Cdelta regulates apoptosis via activation of STAT1. *J Biol Chem*. 2004;279(44):45603–45612. doi: 10.1074/jbc.M407448200

25. Alphonse N, Wanford JJ, Voak AA, et al. A family of conserved bacterial virulence factors dampens interferon responses by blocking calcium signaling. *Cell*. 2022;185(13):2354–2369.e17. doi: 10.1016/j.cell.2022.04.028

26. Hu S, Zhang Y, Yi Q, et al. Time-resolved proteomic profiling reveals compositional and functional transitions across the stress granule life cycle. *Nat Commun*. 2023;14(1):7782. doi: 10.1038/s41467-023-43470-1

27. Thorslund T, Ripplinger A, Hoffmann S, et al. Histone H1 couples initiation and amplification of ubiquitin signalling after DNA damage. *Nature*. 2015;527(7578):389–393. doi: 10.1038/nature15401

28. Choudhury NR, Heikel G, Trubitsyna M, et al. RNA-binding activity of TRIM25 is mediated by its PRY/SPRY domain and is required for ubiquitination. *BMC Biol*. 2017;15(1):105. doi: 10.1186/s12915-017-0444-9

29. Hwang JY, Jung S, Kook TL, et al. rMAPS2: an update of the RNA map analysis and plotting server for alternative splicing regulation. *Nucleic Acids Res*. 2020;48(W1):W300–W306. doi: 10.1093/nar/gkaa237

30. Yang H, Palmbos PL, Wang L, et al. ATDC (Ataxia Telangiectasia Group D Complementing) promotes radioresistance through an Interaction with the RNF8 ubiquitin ligase. *J Biol Chem*. 2015;290(45):27146–27157. doi: 10.1074/jbc.M115.665489

31. Wang L, Yang H, Palmbos PL, et al. ATDC/TRIM29 phosphorylation by ATM/MAPKAP kinase 2 mediates radioresistance in pancreatic cancer cells. *Cancer Res*. 2014;74(6):1778–1788. doi: 10.1158/0008-5472.CAN-13-2289

32. Yuan Z, Villagra A, Peng L, et al. The ATDC (TRIM29) protein binds p53 and antagonizes p53-mediated functions. *Mol Cell Biol*. 2010;30(12):3004–3015. doi: 10.1128/MCB.01023-09

33. Xing J, Zhang A, Minze LJ, et al. TRIM29 negatively regulates the type I IFN production in response to RNA virus. *J Immunol*. 2018;201(1):183–192. doi: 10.4049/jimmunol.1701569

34. Han X, Du H, Massiah MA. Detection and characterization of the in vitro e3 ligase activity of the human MID1 protein. *J Mol Biol*. 2011;407(4):505–520. doi: 10.1016/j.jmb.2011.01.048

35. Li Q, Lin L, Tong Y, et al. TRIM29 negatively controls antiviral immune response through targeting STING for degradation. *Cell Discov*. 2018;4:13. doi: 10.1038/s41421-018-0010-9

СПИСОК ЛИТЕРАТУРЫ

1. Sultanov R., Mulyukina A., Zubkova O., et al. TP63-TRIM29 axis regulates enhancer methylation and chromosomal instability in prostate cancer // Epigenetics Chromatin. 2024. Vol. 17, N. 1. P. 6. doi: 10.1186/s13072-024-00529-7

2. Masuda Y., Takahashi H., Hatakeyama S. TRIM29 regulates the p63-mediated pathway in cervical cancer cells // Biochim Biophys Acta. 2015. Vol. 1853(10 Pt A). P. 2296–2305. doi: 10.1016/j.bbamcr.2015.05.035

3. Palmbos P.L., Wang Y., Bankhead Iii A., et al. ATDC mediates a TP63-regulated basal cancer invasive program // Oncogene. 2019. Vol. 38, N. 18. P. 3340–3354. doi: 10.1038/s41388-018-0646-9

4. Han Q., Sun M.L., Liu W.S., et al. Upregulated expression of ACTL8 contributes to invasion and metastasis and indicates poor prognosis in colorectal cancer // Onco Targets Ther. 2019. Vol. 12. P. 1749–1763. doi: 10.2147/OTT.S185858

5. Du H., Xu Q., Xiao S., et al. MicroRNA-424-5p acts as a potential biomarker and inhibits proliferation and invasion in hepatocellular carcinoma by targeting TRIM29 // Life Sci. 2019. Vol. 224. P. 1–11. doi: 10.1016/j.lfs.2019.03.028

6. Qiu F., Xiong J.P., Deng J., Xiang X.J. TRIM29 functions as an oncogene in gastric cancer and is regulated by miR-185 // Int J Clin Exp Pathol. 2015. Vol. 8, N. 5. P. 5053–5061.

7. Wang L., Yang H., Abel E.V., et al. ATDC induces an invasive switch in KRAS-induced pancreatic tumorigenesis // Genes Dev. 2015. Vol. 29, N. 2. P. 171–183. doi: 10.1101/gad.253591.114

8. Tang Z.P., Dong Q.Z., Cui Q.Z., et al. Ataxia-telangiectasia group D complementing gene (ATDC) promotes lung cancer cell proliferation by activating NF-κB pathway // PLoS One. 2013. Vol. 8, N. 6. P. e63676. doi: 10.1371/journal.pone.0063676

9. Masuda Y., Takahashi H., Sato S., et al. TRIM29 regulates the assembly of DNA repair proteins into damaged chromatin // Nat Commun. 2015. Vol. 6. P. 7299. doi: 10.1038/ncomms8299

10. Yanagi T., Watanabe M., Hata H., et al. Loss of TRIM29 Alters keratin distribution to promote cell invasion in squamous cell carcinoma // Cancer Res. 2018. Vol. 78, N. 24. P. 6795–6806. doi: 10.1158/0008-5472.CAN-18-1495

11. Xing J., Weng L., Yuan B., et al. Identification of a role for TRIM29 in the control of innate immunity in the respiratory tract // Nat Immunol. 2016. Vol. 17, N. 12. P. 1373–1380. doi: 10.1038/ni1216-1479a Corrected and republished from: Nat Immunol. 2016. Vol. 17, N. 12. P. 1479. doi: 10.1038/ni.3580

12. Wu T., Hu E., Xu S., et al. clusterProfiler 4.0: A universal enrichment tool for interpreting omics data // Innovation (Camb). 2021. Vol. 2, N. 3. P. 100141. doi: 10.1016/j.xinn.2021.100141

13. Watson J., Smith M., Francavilla C., Schwartz J.M. SubcellulaRVis: a web-based tool to simplify and visualise subcellular compartment enrichment // Nucleic Acids Res. 2022. Vol. 50(W1). P. W718–W725. doi: 10.1093/nar/gkac336

14. Dobin A., Davis C.A., Schlesinger F., et al. STAR: ultrafast universal RNA-seq aligner // Bioinformatics. 2013. Vol. 29, N. 1. P. 15–21. doi: 10.1093/bioinformatics/bts635

15. Shen S., Park J.W., Lu Z.X., et al. rMATS: robust and flexible detection of differential alternative splicing from replicate RNA-Seq data // Proc Natl Acad Sci U S A. 2014. Vol. 111, N. 51. P. E5593–E5601. doi: 10.1073/pnas.1419161111

16. Meroni G., Diez-Roux G. TRIM/RBCC, a novel class of 'single protein RING finger' E3 ubiquitin ligases // Bioessays. 2005. Vol. 27, N. 11. P. 1147–1157. doi: 10.1002/bies.20304

17. Sardiello M., Cairo S., Fontanella B., et al. Genomic analysis of the TRIM family reveals two groups of genes with distinct evolutionary properties // BMC Evol Biol. 2008. Vol. 8. P. 225. doi: 10.1186/1471-2148-8-225

18. Cardamone M.D., Krones A., Tanasa B., et al. A protective strategy against hyperinflammatory responses requiring the nontranscriptional actions of GPS2 // Mol Cell. 2012. Vol. 46, N. 1. P. 91–104. doi: 10.1016/j.molcel.2012.01.025

19. Yuan J., Luo K., Zhang L., et al. USP10 regulates p53 localization and stability by deubiquitinating p53 // Cell. 2010. Vol. 140, N. 3. P. 384–396. doi: 10.1016/j.cell.2009.12.032

20. Wikiniyadhanee R., Lerksuthirat T., Stitchantrakul W., et al. TRIM29 is required for efficient recruitment of 53BP1 in response to DNA double-strand breaks in vertebrate cells // FEBS Open Bio. 2020. Vol. 10, N. 10. P. 2055–2071. doi: 10.1002/2211-5463.12954

21. Tan G, Xu F, Song H, et al. Identification of TRIM14 as a type I IFN-stimulated gene controlling hepatitis B virus replication by targeting HBx // Front Immunol. 2018. Vol. 9. P. 1872. doi: 10.3389/fimmu.2018.01872

22. Hoffpauir C.T., Bell S.L., West K.O., et al. TRIM14 Is a key regulator of the type I IFN response during mycobacterium tuberculosis infection // J Immunol. 2020. Vol. 205, N. 1. P. 153–167. doi: 10.4049/jimmunol.1901511

23. Liu B., Liao J., Rao X., et al. Inhibition of Stat1-mediated gene activation by PIAS1 // Proc Natl Acad Sci U S A. 1998. Vol. 95, N. 18. P. 10626–10631. doi: 10.1073/pnas.95.18.10626

24. DeVries T.A., Kalkofen R.L., Matassa A.A., Reyland M.E. Protein kinase Cdelta regulates apoptosis via activation of STAT1 // J Biol Chem. 2004. Vol. 279, N. 44. P. 45603–45612. doi: 10.1074/jbc.M407448200

25. Alphonse N., Wanford J.J., Voak A.A., et al. A family of conserved bacterial virulence factors dampens interferon responses by blocking calcium signaling // Cell. 2022. Vol. 185, N. 13. P. 2354–2369. doi: 10.1016/j.cell.2022.04.028

26. Hu S., Zhang Y., Yi Q., et al. Time-resolved proteomic profiling reveals compositional and functional transitions across the stress granule life cycle // Nat Commun. 2023. Vol. 14, N. 1. P. 7782. doi: 10.1038/s41467-023-43470-1

27. Thorslund T., Ripplinger A., Hoffmann S., et al. Histone H1 couples initiation and amplification of ubiquitin signalling after DNA damage // Nature. 2015. Vol. 527, N. 7578. P. 389–393. doi: 10.1038/nature15401

28. Choudhury N.R., Heikel G., Trubitsyna M., et al. RNA-binding activity of TRIM25 is mediated by its PRY/SPRY domain and is

required for ubiquitination // BMC Biol. 2017. Vol. 15, N. 1. P. 105. doi: 10.1186/s12915-017-0444-9
29. Hwang J.Y., Jung S., Kook T.L., et al. rMAPS2: an update of the RNA map analysis and plotting server for alternative splicing regulation // Nucleic Acids Res. 2020. Vol. 48(W1). P. W300–W306. doi: 10.1093/nar/gkaa237
30. Yang H., Palmbos P.L., Wang L., et al. ATDC (Ataxia Telangiectasia Group D Complementing) promotes radioresistance through an interaction with the RNF8 ubiquitin ligase // J Biol Chem. 2015. Vol. 290, N. 45. P. 27146–27157. doi: 10.1074/jbc.M115.665489
31. Wang L., Yang H., Palmbos P.L., et al. ATDC/TRIM29 phosphorylation by ATM/MAPKAP kinase 2 mediates radioresistance in pancreatic cancer cells // Cancer Res. 2014. Vol. 74, N. 6. P. 1778–1788. doi: 10.1158/0008-5472.CAN-13-2289
32. Yuan Z., Villagra A., Peng L., et al. The ATDC (TRIM29) protein binds p53 and antagonizes p53-mediated functions // Mol Cell Biol. 2010. Vol. 30, N. 12. P. 3004–3015. doi: 10.1128/MCB.01023-09
33. Xing J., Zhang A., Minze L.J., et al. TRIM29 negatively regulates the type I IFN production in response to RNA virus // J Immunol. 2018. Vol. 201, N. 1. P. 183–192. doi: 10.4049/jimmunol.1701569
34. Han X., Du H., Massiah M.A. Detection and characterization of the in vitro e3 ligase activity of the human MID1 protein // J Mol Biol. 2011. Vol. 407, N. 4. P. 505–520. doi: 10.1016/j.jmb.2011.01.048
35. Li Q., Lin L., Tong Y., et al. TRIM29 negatively controls antiviral immune response through targeting STING for degradation // Cell Discov. 2018. Vol. 4. P. 25. doi: 10.1038/s41421-018-0031-4 Corrected and republished from: Cell Discov. 2018. Vol. 4. P. 13. doi: 10.1038/s41421-018-0010-9

AUTHORS' INFO

*** Rinat I. Sultanov,** Cand. Sci. (Biology);
address: 1a Malaya Pirogovskaya street, 119435 Moscow, Russia;
ORCID: 0000-0003-3918-708X;
eLibrary SPIN: 2295-5337;
e-mail: rhenium112@gmail.com

Alina S. Mulyukina;
ORCID: 0009-0005-2053-6157;
e-mail: mulyukina.alina@gmail.com

Victoria O. Shender, Cand. Sci. (Chemistry);
ORCID: 0000-0001-9156-2938;
eLibrary SPIN: 2868-5902;
e-mail: victoria.shender@gmail.com

Maria M. Lukina, Cand. Sci. (Biology);
ORCID: 0000-0003-1374-8571;
eLibrary SPIN: 5113-0571;
e-mail: kuznetsova.m.m@yandex.ru

Maria A. Lagarkova, Dr. Sci. (Biology),
Corresponding Member of the Russian Academy of Sciences;
ORCID: 0000-0001-9594-1134;
eLibrary SPIN: 4315-1701;
e-mail: lagar@rcpcm.org

Georgij P. Arapidi, Cand. Sci. (Biology);
ORCID: 0000-0003-2323-1859;
eLibrary SPIN: 5871-4438;
e-mail: arapidi@gmail.com

* Corresponding author / Автор, ответственный за переписку

ОБ АВТОРАХ

*** Султанов Ринат Илгизович,** канд. биол. наук;
адрес: Россия, 119435, Москва, ул. Малая Пироговская, д. 1а;
ORCID: 0000-0003-3918-708X;
eLibrary SPIN: 2295-5337;
e-mail: rhenium112@gmail.com

Мулюкина Алина Сергеевна;
ORCID: 0009-0005-2053-6157;
e-mail: mulyukina.alina@gmail.com

Шендер Виктория Олеговна, канд. хим. наук;
ORCID: 0000-0001-9156-2938;
eLibrary SPIN: 2868-5902;
e-mail: victoria.shender@gmail.com

Лукина Мария Максимовна, канд. биол. наук;
ORCID: 0000-0003-1374-8571;
eLibrary SPIN: 5113-0571;
e-mail: kuznetsova.m.m@yandex.ru

Лагарькова Мария Андреевна, д-р биол. наук,
член-корреспондент РАН;
ORCID: 0000-0001-9594-1134;
eLibrary SPIN: 4315-1701;
e-mail: lagar@rcpcm.org

Арапиди Георгий Павлович, канд. биол. наук;
ORCID: 0000-0003-2323-1859;
eLibrary SPIN: 5871-4438;
e-mail: arapidi@gmail.com